Netsu Sokutei **45** (4), 138-142 (2018)

Article

Calorimetric Analysis of the Effects of Mutations on the Function and Stability of *Streptococcal* Protein G as an Affinity Ligand for Antibody Fragments

Shinichi Yoshida [a,b]

[a] Biotechnology Research Laboratories, KANEKA Corporation,
[b] Manufacturing Technology Association of Biologics

(Received Aug. 2, 2018; Accepted Aug. 24, 2018)

Streptococcal protein G (SpG) is a bacterial surface protein, binding mainly to the Fc (high affinity) and Fab (low affinity) regions of immunoglobulins. The SpG-immobilized affinity chromatography resin is useful for the purification of antibodies. Improvement of the affinity of SpG to Fab enhances its application to the purification of Fab-based antibody fragments. We found four important mutations of SpG, improving its affinity for Fab through affinity maturation using a ribosomal display system. In this article, we discuss the thermodynamic effects of these mutations on the function and stability of SpG as an affinity ligand using calorimetric measurements. Isothermal titration calorimetry analysis elucidated the quantitative enthalpic/entropic contributions of these individual mutations on the interaction of SpG with Fab. In addition, differential scanning calorimetry analysis revealed the destabilizing effects of these mutations on the thermodynamic stability of SpG. These calorimetric analyses may contribute to the current understanding of the mechanism of action of such mutations and further refinement of affinity ligands through protein engineering.
Keywords: protein G, affinity ligand, immunoglobulin, protein engineering

1. Introduction

A number of Gram-positive bacteria express cell surface-anchored binders for different host-specific serum proteins, especially immunoglobulins (Ig).[1,2] One of these bacterial proteins, Streptococcal protein G (SpG), was isolated from C and G groups of *Streptococcus*. SpG binds to the Fc (high affinity) and Fab (low affinity) regions of IgG. In SpG, there are several IgG-binding domains composed of approximately 50 amino acids. The global fold of the IgG-binding domains of SpG consists of a four-stranded β-sheet spanned by an α-helix [**Fig.1**]. [3]

Affinity chromatography depends on specific and reversible binding between a target to be purified and its binder, termed affinity ligand, immobilized on a stationary phase support. Bacterial proteins such as SpG are useful as affinity ligands for the purification of antibodies.[2,4] The IgG-binding domains of SpG have low affinity to Fab and are unable to maintain adsorption during the wash steps to remove impurities. Therefore, the purification of antibody fragments not including Fc regions, through the use of SpG-immobilized resin, is challenging. We engineered the IgG-binding domain of SpG, enhancing its affinity to Fab, to develop a new useful tool for the purification of antibody fragments.

IgG-binding domains of SpG with higher affinity to Fab were selected through affinity maturation using a ribosomal display system. Details of this study will be published elsewhere. An analysis of the amino acid sequences of selected binders with high affinity to Fab regions, revealed several mutations in almost all of selected binders. These mutations (*i.e.*, K13T, E19I, F30L and Y33F) may play an important role in enhancing the affinity of the IgG-binding domains of SpG to Fab regions.

The purpose of the present study was to examine the thermodynamic effects of these mutations of the IgG-binding domains of SpG using a calorimetric method. This study may improve the current understanding of the enhancing mechanism for the binding ability of SpG to Fab regions. In addition, the effects of these mutations on the stability of SpG were investigated using a different calorimetric method.

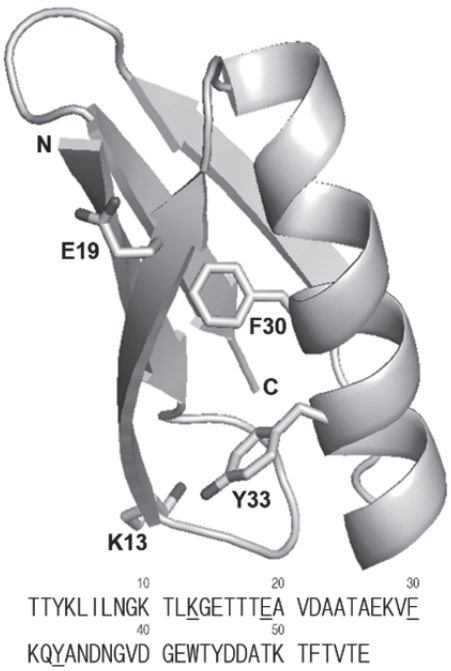

Fig.1 The Three-dimensional structural model of the immunoglobulin binding domain of SpG used in this study, the B1 domain of SpG (SpG-B1). This model was constructed by using PDB coordinates (1IGC) [18] as a template structure. The side chains of residues mutated in this study are shown as a stick model. This figure was generated by PyMOL (Schrödinger). The sequence of wild-type SpG-B1 is also shown.

2. Materials and Methods

2.1 Expression plasmid

In this study, the B1 domain of SpG (SpG-B1) derived from strain GX7809 was used as the wild-type IgG-binding domain of SpG. The amino acid sequence in which Asp at the first position of SpG-B1 is substituted by Thr, which is matched to the N-terminus amino acid of the B2 domain of SpG. The DNA encoding the wild-type SpG-B1 and its mutants was prepared through ligation of two double-stranded DNA fragments, designated as f1 or f2, cut with restriction enzymes, and inserted into the multicloning site of the expression vector pGEX-6P (GE Healthcare) [**Fig.2, Table 1**].

The two double-stranded DNA fragments were prepared through extension of two single-stranded oligo-DNA fragments, designated as f1-1, f1-2, f2-1, and f2-2, containing a complementary region of approximately 10 bases with each other using overlap extension polymerase chain reaction (PCR) to prepare the desired double-stranded DNA fragment f1 or f2, respectively. Single-stranded oligo-DNAs were synthesized by Eurofin Genomics. A DNA encoding the wild-type SpG-B1 and its mutants were prepared to connect two kinds of double-stranded DNAs having the same restriction enzyme site. Regarding the mutants of SpG-B1, for example, an expression plasmid for the K13T mutant of SpG-B1 was prepared using f1-2-K13T instead of f1-2-Wild. Single-stranded oligo-DNAs were synthesized by Eurofin Genomics. The overlap extension PCR was performed using Blend Taq Plus polymerase (Toyobo). The PCR product was subjected to agarose electrophoresis and a double-stranded DNA was extracted by cutting out the target band using the restriction enzymes *Bam*HI and *Eco*52I in the case of DNA fragment f1, or *Eco*52I and *Eco*RI in the case of DNA fragment f1 (Takara). Subsequently, these two double-stranded DNA fragments were subcloned at the *Bam*HI/*Eco*RI site in the multicloning site of the plasmid vector pGEX-6P-1. The ligation reaction in the subcloning experiment was carried out using Ligation High (Toyobo).

2.2 Protein expression

Protein expression was carried out by transformation of each expression plasmid into *Escherichia coli* (*E. coli*) HB101 (Takara). Proteins were expressed as glutathione S-transferase (GST) fusion proteins using the vector pGEX-6P. Each transformed cell was cultured in LB medium containing ampicillin at 37 °C overnight. The culture fluid was inoculated in an approximately 100-fold volume of 2xYT medium containing ampicillin and cultured at 30 °C for approximately three hours. Isopropyl-1-thio-β-D-galactoside was then added to a final concentration of 0.2 mM, followed by culture at 30 °C for 18 hours. Cells were suspended in PBS (pH 7.4) containing 0.5 mM EDTA and the suspended cells were disrupted using a probe sonicator. Following protein purification, chromatography was performed using an AKTAprime plus system (GE Healthcare). The supernatant was separated from the sonicated mixtures through centrifugation and was transferred to a GSTrap HP column (GE Healthcare) equilibrated with 20 mM sodium phosphate (pH 7.4) containing 0.15 M NaCl. After washing in equilibrating buffer, the target protein was eluted using 50 mM Tris-HCl (pH 8.0) containing 20 mM glutathione. The GST-tag was cleaved by the addition of PreScission Protease (GE Healthcare) to the eluted fraction. The target protein was separated from the GST-tag through gel-filtration chromatography using a Superdex™ 75 column (GE Healthcare) with 20 mM NaH_2PO_4-Na_2HPO_4, 150 mM NaCl, pH 7.4.

2.3 Fab fragments

The Fab fragment was prepared through cleavage of monoclonal IgGs as starting material into a Fab fragment and an Fc fragment using papain, followed by separation and purification of the Fab fragment. The formulation of monoclonal IgG was dissolved in a papain digestion buffer (0.1 M AcOH-AcONa, 2 mM EDTA, 1 mM cysteine, pH 5.5). Six monoclonal IgGs (*i.e.*, palivizumab, infliximab, cetuximab, trastuzumab, omalizumab, and denosumab) were used. Papain agarose from papaya latex (Sigma) was added to the solution and the mixture was incubated at 37 °C for approximately 8 hours under continuous mixing using a rotator. The Fab fragment was collected from the flow-through fractions using affinity chromatography with a KanCapA™ column (Kaneka). The separated Fab solution was purified by gel filtration chromatography using a Superdex™ 75 column with 20 mM NaH_2PO_4-Na_2HPO_4, 150 mM NaCl, pH 7.4.

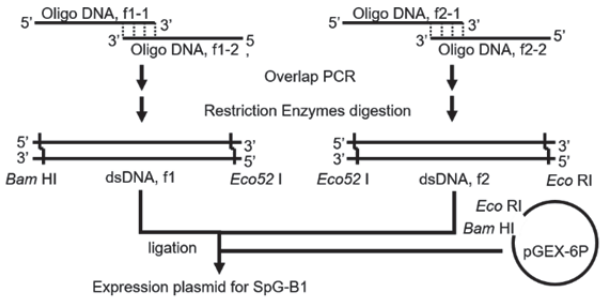

Fig.2 Schematic flow diagram. Schematic representation of the preparation for an expression plasmid of SpG-B1.

Table 1 Sequence of oligo-DNA fragments.

Name	Sequence
f1-1-Wild	5'-cgtggatcca ccacctacaa actgatcctg aacggtaaga ccctgaaagg tgaaaccacc-3'
f1-2-Wild	5'-ttcggccgta gcagcgtcaa cagcttcggt ggtggtttca cctttcaggg tcttaccgtt-3'
f1-2-K13T	5'-ttcggccgta gcagcgtcaa cagcttcggt ggtggtttca cctGtcaggg tcttaccgtt-3'
f1-2-E19I	5'-ttcggccgta gcagcgtcaa cagctATggt ggtggtttca cctttcaggg tcttaccgtt-3'
f1-2-K13T/E19I	5'-ttcggccgta gcagcgtcaa cagctATggt ggtggtttca cctGtcaggg tcttaccgtt-3'
f2-1-Wild	5'-ctacggccga aaaagtgttc aaacagtacg ctaacgacaa cggtgtcgac ggtgaatgga cctacgacga -3'
f2-1-F30L	5'-ctacggccga aaaagtgCtc aaacagtacg ctaacgacaa cggtgtcgac ggtgaatgga cctacgacga -3'
f2-1-Y33F	5'-ctacggccga aaaagtgttc aaacagtTcg ctaacgacaa cggtgtcgac ggtgaatgga cctacgacga -3'
f2-1-F30L/Y33F	5'-ctacggccga aaaagtgCtc aaacagtTcg ctaacgacaa cggtgtcgac ggtgaatgga cctacgacga -3'
f2-2-Wild	5'-cgatgaattc tattcggtaa ccgtgaaggt tttggtagcg tcgtcgtagg tccattcacc gtcgacaccg -3'

2.4 Surface plasmon resonance (SPR)

The kinetic parameters between wild-type or mutant SpG-B1 and Fab were evaluated using the SPR-based sensor BIACORE® 3000 (GE Healthcare). Each of the six Fabs was immobilized by amine coupling on the carboxylated dextran surface of a CM5 sensor chip using N-hydroxysuccinimide (NHS) and N-ethyl-N'-(3-dimethylaminopropyl) carbodiimide (EDC) chemistry according to the manufacturer's protocol. A

reference lane was chemically blocked with ethanolamine immediately after activation with NHS/EDC. A 1 mg mL^{-1} Fab solution was diluted in 10 mM sodium acetate (pH 4.5) prior to use in this immobilization process. To analyze the Fab-binding affinity, solutions of four different protein concentrations (from 10 to 10000 nM) were prepared for each protein using a running buffer (20 mM NaH_2PO_4-Na_2HPO_4, 150 mM NaCl, 0.005 % P-20, pH 7.4). Each of the SpG-B1 solutions was applied onto the sensor chip at a flow rate of 20 μL min^{-1}, and 40 mM NaOH was used to regenerate the surface. All experiments were performed at 25 °C. The data were analyzed using the BIA evaluation software.

2.5 Isothermal titration calorimetry (ITC)

The thermodynamic parameters between wild-type or mutant SpG-B1 and Fab prepared from omalizumab were evaluated using an isothermal titration calorimeter, Nano ITC LV (TA instruments). All sample solutions were dialyzed with 20 mM NaH_2PO_4-Na_2HPO_4, 150 mM NaCl, pH 7.4 and degassed prior to the titrations. Each 100 μM of the SpG-B1 solution was titrated into the 20 μM Fab solution. Each titration consisted of 2 μL every 3 min. All experiments were performed at 25 °C. The heat for each injection was subtracted from that of the dilution of the wild-type SpG-B1 into the experimental buffer. Each corrected heat was divided by the moles of SpG-B1 injected and analyzed using the NanoAnalyze (TA instruments).

2.6 Differential scanning calorimetry (DSC)

The unfolding transition midpoint temperature of each SpG-B1 was evaluated using DSC, Nano DSC (TA instruments). The temperature was increased from 20 to 120 °C at a scan rate 1 °C min^{-1}. The scans were performed in 20 mM NaH_2PO_4-Na_2HPO_4, 150 mM NaCl, pH 7.4 at a final protein concentration of 0.25 mg mL^{-1}. Each corrected heat was subtracted from that of the experimental buffer and was analyzed using the NanoAnalyze (TA instruments).

3. Results and Discussion

We evaluated the effects of the K13T, E19I, F30L, and Y33F mutations, identified through affinity maturation using a ribosomal display, on the function and stability of the IgG-binding domain of SpG *in vitro*. The B1 domain of SpG (SpG-B1) derived from the strain GX7809 was used as the wild-type IgG-binding domain of SpG, as widely used in previous studies investigating the IgG-binding domain of SpG.[5,6] However similar tendency should be expected when using other IgG-binding domains of SpG because of their significantly high sequential identities. Wild-type and 15 mutants of SpG-B1 were prepared to assess the effect of these four mutations individually and in combination.

The SPR method allows the measurement of biospecific interactions in real time as changes in mass concentration on a sensor surface.[7,8] In this experiment, the wild-type and each mutant of SpG-B1 was passed through the Fab-immobilized surface. The binding constant (K_A) were calculated for the wild-type and each mutant of SpG-B1 in an identical manner. The K_A values for binding of wild-type SpG-B1 to the Fab region ranged between 0.6-1.2 × 10^6 M^{-1} which is similar to values evaluated by SPR experiment in a previous report.[9] The average value of the ratio of the K_A values for each mutant to wild-type for six Fabs were represented using the decadic logarithm [**Fig.3**].

The binding constant of every mutant of SpG-B1 having a single mutation, K13T, E19I, F30L or Y33F, had almost doubled compared with that of the wild-type. Multiple mutations of these four mutations to wild-type SpG-B1 seems to act in an additive manner for the enhancement of the binding constant, resulting in the highest K_A value of the mutant which all the mutations were introduced. However, it is difficult to predict the mechanism of action of these mutational effects based only on the kinetic analysis.

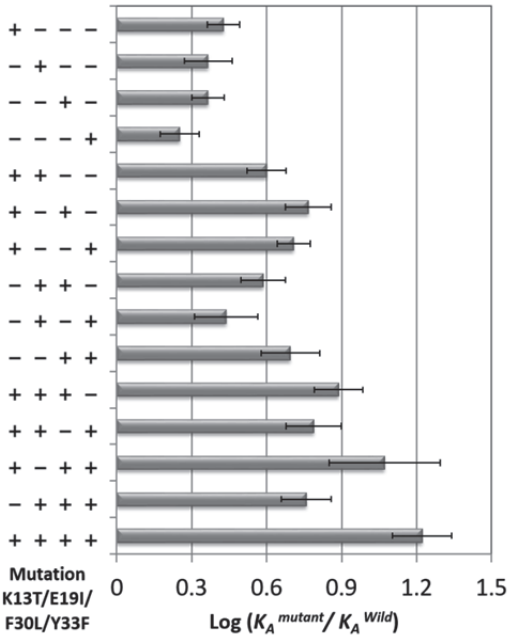

Fig.3 The average value of the ratio of the K_A of each mutant to wild-type for every Fab region. A 1:1 Langmuir model was used to calculate values of the K_A.

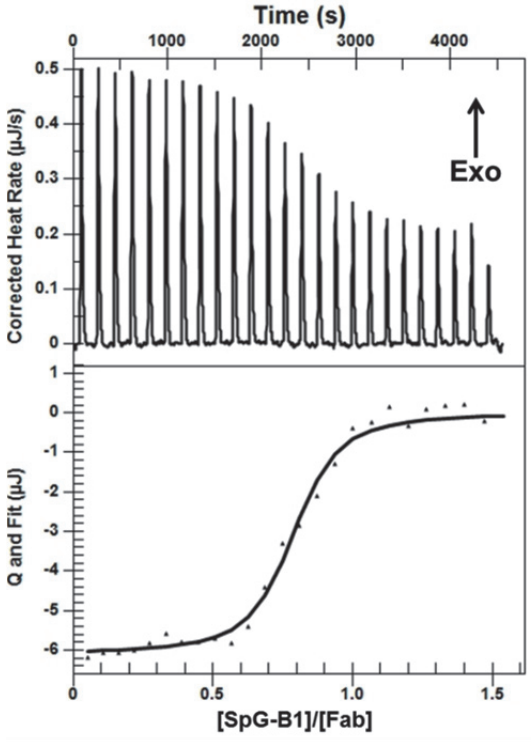

Fig.4 ITC thermogram and binding isotherm for the interaction between Fab and SpG-B1 mutant (K13T/E19I/ F30L/Y33F). A general 1:1 binding model was used for the curve fitting.

ITC was selected to further analysis the effects of these mutations on the binding ability of SpG-B1 to Fab. ITC is a unique method to determine thermodynamic binding parameters for molecular interactions.[10] Experiments were performed for a single type of Fab because ITC is not suitable for high-throughput experiments. An exothermic heat pulse was observed after each injection of SpG-B1 to Fab [**Fig.4**]. The K_A

value for the interaction between wild-type SpG-B1 and Fab, prepared from omalizumab, was 1.5×10^6 M^{-1}, which is consistent with the value of 1.1×10^6 M^{-1}obtained from the SPR-based experiment. The enhancement of the affinity of SpG-B1 to Fab through the introduction of mutations in the SpG-B1 was also similar to that observed in the SPR-based experiment. The thermodynamic parameters were calculated for the interactions between wild-type or each mutant of SpG-B1 and Fab. The enthalpy change (ΔH) is obtained directly from the experimental data, while the changes in Gibbs free energy (ΔG) and entropy (ΔS, $-T\Delta S$) are calculated from known thermodynamic relations. The value of ΔH, ΔG and $-T\Delta S$ for wild-type SpG-B1 are −25.5 kJ mol^{-1}, −35.3 kJ mol^{-1} and −9.7 kJ/mol, respectively. These thermodynamic parameters of the interaction between wild-type SpG-B1 and Fab are similar to those reported in a previous study.[11] Regarding the thermodynamic parameters of each SpG-B1 mutant, the difference values versus those of the wild-type SpG-B1 are represented as a bar graph [**Fig.5**].

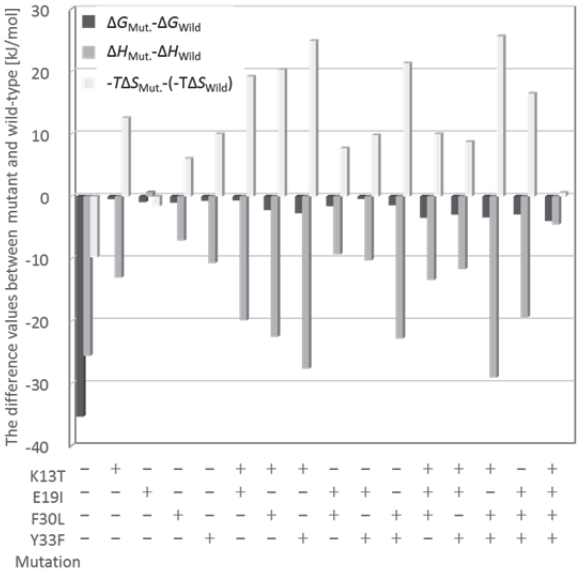

Fig.5 Difference values of thermodynamic parameters of binding for each SpG-B1 mutant to Fab versus that of the wild-type.

For this graphic representation, all the favorable thermodynamic parameters are represented by a negative value.[12] Introducing these mutations to wild-type SpG-B1 affects the absolute values of ΔG positively. This trend corresponds to the trend of K_A observed in the SPR-based experiment, which is not in conflict with the proportional relation between ΔG and K_A. [10] The binding of each SpG-B1 mutant to Fab is more enthalpy-driven than that of wild-type SpG-B1. However, only the E19I mutation contributes to entropic change more favorably (more negatively) than the enthalpic one. The favorable enthalpic contributions of the K13T, F30L, and Y33F mutations are enhanced in an additive manner in the case of containing none of the E19I mutation in SpG-B1. The entropic contribution becomes unfavorable when the E19I mutation is combined with other mutations in SpG-B1. It is noteworthy that the entropic loss is significantly suppressed when all four mutations are introduced. Although the enthalpic/entropic contributions of the mutations of SpG-B1 to its interaction with Fab are complicated, this comprehensive analysis may be useful in expanding our thermodynamic understanding of biological interactions.

The effects of mutations on the thermodynamic stability of SpG-B1 were also analyzed using DSC. DSC is the main technique used in the characterization of the thermal stability of proteins.[13] Thermodynamic stability is important for affinity ligands because an affinity resin is used for prolonged period of time at room temperature in various settings.[4] A previous report suggested that thermodynamic stability is responsible for the alkaline stability required for cleaning and sanitization.[14,15] The thermal unfolding transitions of wild-type and mutants of SpG-B1 were measured under physiological conditions. Unfortunately, the calorimetric enthalpy of unfolding (ΔH) and the heat capacity changes on unfolding (ΔC_p) were not determined because of an aggregation of SpG-B1 at a high temperature > 90 °C. However, when the unfolding transition midpoint temperature (T_m) of the SpG-B1 mutant was relatively low (approximately 60-65 °C), the baseline of the unfolding state was slightly observed at 85-90 °C [**Fig.6**].

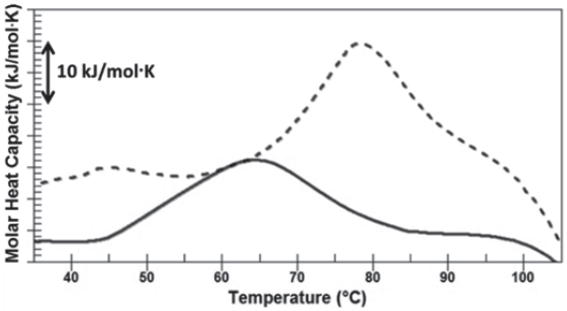

Fig.6 Differential scanning calorimetry heating curves for the thermal denaturation of the wild-type of SpG-B1 (broken line) and its mutant (K13T/E19I/F30L/Y33F, solid line).

However, all the T_m values of the wild-type and mutants of SpG-B1 were evaluated because the single symmetrical unfolding transition was observed in every measurement. The T_m value of 78.5 °C observed for wild-type SpG-B1 is similar to values obtained through circular dichroism experiments in a previous study.[16,17] Regarding the thermodynamic parameters of each SpG-B1 mutant, the difference values from those reported for wild-type SpG-B1 are represented as a bar graph [**Fig.7**]. There were no mutants showing significantly higher values of T_m than that reported for wild-type. Moreover, the T_m value of nearly three-quarters of the mutants was decreased by > 5 °C compared with that of the wild-type. The K13T and F30L mutations destabilize the thermodynamic stability of SpG-B1, whereas the E19I and Y33F mutations do not exert a destabilizing effect. The destabilization effect of these mutations is likely to be independent. For this reason, this effect is maximized when introducing the K13T/F30L double mutation to SpG-B1. Although the thermodynamic stability of SpG-B1 is not essential for its function as an affinity ligand, this information may be important to care its weakness.

In terms of three-dimensional structure of the SpG/Fab complex, a second β-strand forms an extended β-sheet with the β-sheet of Fab and main-chain atoms of SpG-B1 mainly relate to this interaction. [18] The Lys-13 residue is located on the second β-strand of SpG-B1and binding interface to Fab [**Fig.8**]. From the results of the ITC analysis, the substitution of Asp by Thr may form a new hydrogen bond which the hydroxyl group of Thr is related to. According to the results of the DSC, the change of basic side-chain to a neutral chain may result in loss of important electrostatic interactions on the surface of SpG-B1. The Glu-19 residue is located on loop region of SpG-B1 and is a little apart from the binding interface to Fab. Although it is difficult to illustrate results of this study, the change of the acidic side-chain to the large hydrophobic side-chain may simply contribute to the enhancement of a hydrophobic interaction. The Phe-30 residue is located on the α-helix and its side-chain is buried in a hydrophobic core region of SpG-B1. A previous

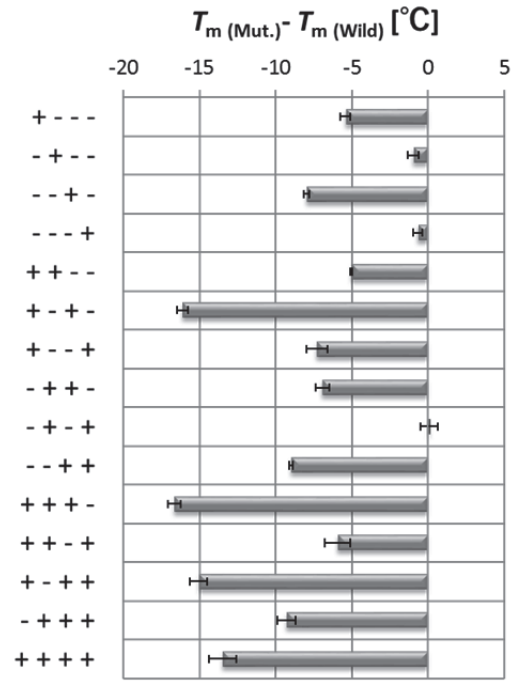

Fig.7 Difference values of T_m for each of the SpG-B1 mutants. Standard errors from the fit were estimated using NanoAnalyze (TA instruments).

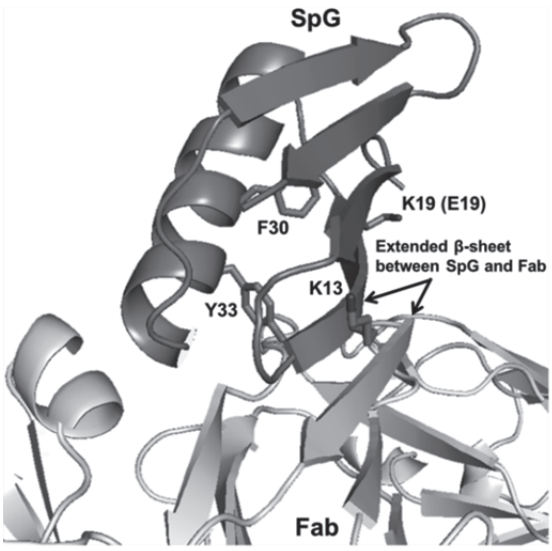

Fig.8 The three-dimensional structure of the SpG/Fab complex (PDB:1IGC). [18] The SpG-B2 was used in this X-ray crystal structure analysis. The side chains of residues mutated in this study are shown as a stick model. The amino acid at position-19 is Lys in SpG-B2. This figure was generated by PyMOL (Schrödinger).

study showed that the F30L mutation alters subtly the overall structure of SpG-B1.[19,20] Therefore, although it is also difficult to simplify the effect by this mutation, it is no wonder to result in both enthalpic contributions to the binding of SpG-B1 to Fab and destabilization of the thermodynamic stability of SpG-B1. Regarding the Tyr-33 residues, a hydrogen bond is observed in the crystal structure of the SpG/Fab complex between the hydroxyl group of the side-chain of Tyr-33 in SpG-B1 and the main-chain carbonyl group. Although the substitution to Phe is expected to result in loss of this hydrogen bond, the results of ITC analysis were unexpected. The Y33F mutation may positively affect the extended β-sheet between the SpG-B1 and Fab because the side-chain of Tyr-33 is located near the main-chain structure of the second β-strand. Thus, the thermodynamic analysis may support a prediction of the mechanism of action through mutation although it is not always to be understood.

4. Conclusion

This study demonstrated that the calorimetric analysis may expand the current understanding of the effects of mutations on proteins. All the mutations of SpG-B1 (K13T, E19I, F30L, and Y33F) were found to enhance its binding to Fab independently and in a synergistic manner. ITC analysis revealed differences in the enthalpic/entropic contributions of individual mutations to the interaction between SpG-B1 and Fab.

Moreover, it was shown that the enthalpic/entropic contributions of multiple mutations may not always act in an additive manner. DSC analysis provided new data on the effects of these mutations on the thermodynamic stability of SpG-B1. We believe that thermodynamic analysis of the effects of mutations may advance the further engineering of proteins as affinity ligands.

Acknowledgement

This research was supported in part by the developing key technologies for discovering and manufacturing pharmaceuticals used for next-generation treatments and diagnoses both from the Ministry of Economy, Trade and Industry, Japan (METI) and from Japan Agency for Medical Research and Development (AMED). The authors would like to thank Enago (www.enago.jp) for the English language review.

References

1) R. Nezlin and V. Ghetie, *Adv. Immunol.* **82**, 155-215 (2004).
2) T. Bostrom, *et al., Protein Purification (Chapter 5)*, In Tech (2012).
3) A. Achari, *et al.*, *Biochemistry* **31**, 10449-10457 (1992)
4) S. Arora, *et al*., *Methods* **116**, 84-94 (2017).
5) S. R. Fahnestock, *et al*., *J. Bacteriol.* **167**, 870-880 (1986).
6) A. Olsson, *et al.*, *Eur. J. Biochem.* **168**, 319-324 (1987).
7) H. N. Daghestani, *et al.*, *Sensors* **10**, 9630-9646 (2010).
8) H. H. Nguyen, *et al., Sensors* **15**, 10481-10510 (2015).
9) T. Sagawa, *et al*., *Mol. Immunol.* **42**, 9-18 (2005).
10) M. S. Atri, *et al*., *Phy. Chem. Res.* **3**, 319-330 (2015).
11) L. N. Lund *et al.*, *J. Mol. Recognit.* **24**, 945-952 (2011).
12) A. I. Dragan, *et al.*, *Eur. Biophys. J.* **46**, 301-308 (2017).
13) G. Bruylants, *et al.*, *Curr. Med. Chem.* **12**, 2011-2020 (2005).
14) S. Gulich, *et al.*, *Protein Eng.* **15**, 835-842 (2002).
15) B. Palmer, *et al.*, *J. Biotechnol.* **134**, 222-230 (2008).
16) P. Alexander, *et al.*, *Biochemistry* **31**, 3597-3603 (1992).
17) S. Honda, *et al*., *Biochemistry* **38**, 1203-1213 (1999).
18) J. P. Derrick and D.B. Wigley, *J. Mol. Biol.* **243**, 906-918 (1994).
19) A. Su and S. L. Mayo, *Protein Sci.* **6**, 1701-1707 (1997).
20) S. A. Ross et al., *Protein Sci.* **10**, 450-454 (2001).

Shinichi Yoshida

E-mail: Shinichi.Yoshida@kaneka.co.jp